Near-Surface Dynamics of Sheared Polymer Melts Using ATR/FTIR

Geoffrey M. Wise, Morton M. Denn, and Alexis T. Bell
Materials Sciences Division, Lawrence Berkeley National Laboratory and
Dept. of Chemical Engineering, University of California at Berkeley, Berkeley, CA 94720

Using attenuated total-reflectance infrared spectroscopy (ATR/FTIR), the concentration of deuterated polybutadiene near the surface of a flat zinc selenide crystal was followed as it was replaced by ordinary polybutadiene by flow and diffusion. Experiments were performed in the melt, both below ($M \sim 1,500$) and above ($M \sim 15,000$) the entanglement threshold. The decay profiles agree well with a finite-element simulation of the system. In contrast to previous investigations of C_{16}'s, the decay profiles of both unentangled and entangled polybutadienes are consistent with a uniform diffusivity in the near-wall region.

Introduction

The anomalous flow behavior of polymer melts at high stresses is often the limiting factor for high throughputs in polymer processing. At wall shear stresses above 10^5 Pa, extruded polymer melts may exhibit apparent wall slip and distorted extrudate surfaces and shapes (*sharkskin, melt fracture*). Polymer molecular-weight distributions, melt viscoelasticity, energetic interactions with the die surface, and surface topology can all influence the onset and severity of slip and extrudate distortions (for reviews, see Denn, 1990; Larson, 1992). It has been suggested (Brochard and de Gennes, 1992; Wang et al., 1996) that wall slip and extrudate distortion may be due to unusual behavior of the near-surface chains. However, this connection between near-wall chain dynamics and macroscopic flow behavior has not been clearly elucidated, in part because the dynamics of near-surface chains under flow conditions are still poorly understood.

The near-surface dynamics of quiescent polymer melts have been studied theoretically and experimentally. Molecular-dynamics and Monte Carlo simulations have suggested that short (5-mer to 20-mer) polymer chains close to a planar surface have a reduced mobility normal to that surface, even in the absence of surface energetics (Mansfield and Theodorou, 1989; Pan and Bitsanis, 1993; Bitsanis and ten Brinke, 1993). The effect of the wall (densification and preferential alignment of bonds parallel to the wall) may reduce the transverse diffusivity of near-surface chains by a factor between 2 and 10 (Mansfield and Theodorou, 1989; Bitsanis and Pan, 1993). The simulations also indicated that the dynamics are slowed only in a small interfacial region a few segments wide.

Previous investigations in our laboratory using attenuated total-reflection infrared spectroscopy (ATR/FTIR) (Dietsche et al., 1995; David et al., 1995) demonstrated the existence of surprisingly-long time scales for the diffusion of linear oligomers (C_{16}'s) away from a flat surface under mild flow conditions. Although the most marked departure from simple diffusion occurred with hexadecane functionalized by polar groups (carboxylic acids, alcohols, amines), anomalously slow diffusion occurred even in the case of the interdiffusion of hexadecane and 1-hexadecene, which should have weak interactions with the surfaces used in these experiments. The experiments suggested that slow dynamics occur over a near-surface region of depth 5–10 nm, which is greater than found for simulations of chains of similar length. Furthermore, the near-surface slowdown was much more pronounced than predicted by simulations, even for temperatures as high as 70°C above the melting points of the diffusants.

For longer chains, simulations (Pan and Bitsanis, 1993; Shaffer, 1996) have demonstrated that the effect of a nonattractive wall on the near-surface dynamics should become negligible. The decreasing importance of the surface on dynamics with increasing molecular weight can be reasoned as follows: As the chain length increases, the average length of a "train" of polymer segments near the surface asymptotically approaches a constant value (Kumar and Russell, 1991). Thus, for increasing chain length, the surface desorption time of the trains remains relatively constant, while the relaxation

Correspondence concerning this article should be addressed to M. M. Denn.

time of the entire chain increases (linearly with chain length for unentangled chains, and as [chain length]$^{3.4}$ for entangled chains).

To our knowledge, there have been no experimental studies on the near-surface dynamics of polymer melts near nonattractive surfaces. However, recent dynamic SIMS experiments by Zheng and coworkers (1995) with thin, high molecular-weight polystyrene layers show that the diffusivity normal to a strongly attractive surface is reduced from the bulk diffusivity. Zheng and coworkers attribute the hundredfold reduced mobility relative to the vacuum interface to additional friction from wall–monomer enthalpic interactions, not from conformational changes induced by the presence of the wall. They also found that less-attractive surfaces reduced the near-wall diffusion coefficient by a much smaller factor (~ 3) than did the very attractive surfaces.

The purpose of the present study was to determine if the extremely slow near-surface dynamics seen in previous work with C_{16}'s would occur with longer, noncrystallizable chains near a nonattractive surface under mild flow conditions. As a model system, we chose to use isotopically labeled polybutadienes with high 1,4 enchainment. Mixtures of deuterated and ordinary 1,4-polybutadienes have been reported to be completely miscible up to a molecular weight near 150,000–200,000 g/mol at room temperature (Jinnai et al., 1993; Bates and Wiltzius, 1989), allowing us to neglect chemical nonidealities of the blend. M_e, the molecular weight between entanglements, is only about 1,800 g/mol for 1,4 polybutadiene (Colby et al., 1987; Fetters et al., 1994), allowing us to study both unentangled and entangled polymers while avoiding the difficulties associated with synthesizing high-molecular-weight polymers. Furthermore, deuterium-labeled polymers have a relatively strong absorption band at 2,210 cm^{-1} in an otherwise "quiet" region of the IR spectrum. Finally, these polymers are completely amorphous (Carella et al., 1984), enabling us to study near-surface dynamics of molecules that have no tendency to crystallize.

Polymerization

Both ordinary polybutadiene (hereafter referred to as h-PB) and deuterated polybutadiene (d-PB) were synthesized in our laboratory using standard vacuum/inert-atmosphere techniques (Ndoni et al., 1995). Polymerizations were carried out with monomer concentrations near 10% in rigorously purified benzene at 50°C. Anisole was added to the reaction mixture in a 2:1 ratio to *n*-butyllithium to increase the rate of initiation (Bates et al., 1984). The monomers were purified by vacuum distillation through a packed column of 13X molecular sieves before condensation and introduction into the reaction mixture. All chemicals were purchased from Aldrich Chemical Co. except for *d*6-butadiene, which was obtained from Cambridge Isotope Laboratories.

The polymerization reactions were terminated with degassed methanol. The polymers were precipitated and washed in methanol, then dried for several days in a vacuum oven at 35°C, after which they were stored at −5°C under nitrogen until use. We found no broadening of molecular-weight distributions under storage or experimental conditions. Because we were only able to make about 80 g of polymer per batch, the h-PBs were actually mixtures of three to four batches of similar molecular weights.

Table 1. Molecular Properties of Synthesized Polymers

	Size		Microstructure (%)		
Polymer	x_n	M_w/M_n	1,4 cis	1,4 trans	1,2 (vinyl)
h-PB1	29.4	1.06	34	49	17
d-PB1	28.7	1.05			
h-PB2	233	1.05	28	39	33
d-PB2	270	1.12			
GY2600	~ 48 *	1.08*	38*	55*	07*
	44.4**	1.09**	37**	54**	09**

*Data supplied by manufacturer.
**Determined by the authors.

Characterization

Molecular-weight determination

The molecular-weight distributions (MWDs) were determined in a Waters 410 size-exclusion chromatograph (SEC), using tetrahydrofuran at 35°C as the mobile phase (Table 1). The distributions were calibrated with narrow-MWD 1,4-polybutadiene standards purchased from Goodyear and Scientific Polymer Products. It was assumed that the substitution of deuterons for protons did not change the elution time of the samples. The polydispersities of the synthesized polymers were not corrected for axial dispersion. The degree of polymerization, x_n, is defined as the average number of C_4H_6 repeat units per chain. M_w and M_n are the weight- and number-average molecular weights, respectively.

Microstructure

We estimated the microstructure of the h-PB samples by ATR/FTIR using published molar absorptivities (Brandrup and Immergut, 1987) corrected for ATR absorption (Mirabella, 1993). Based on published studies (Atkin et al., 1984; van der Velden et al., 1990), it is expected that the h-PBs and the d-PBs have similar proportions of *cis*, vinyl, and *trans* linkages.

The results of the molecular characterizations are shown in Table 1. As a check on the accuracy of the molecular-weight and microstructure determinations, our characterization of a Goodyear polybutadiene is compared to the manufacturer's data.

Surface energetics

For the purpose of characterizing the experimental surface as being strongly or weakly attractive for the polymers under study, we wished to calculate or measure the interaction energy of the zinc selenide–polybutadiene interface. Although there have been many theoretical and experimental articles on the interaction strengths of polymers, alkanes, and alkenes with metals, we were unable to find any published work on the interaction of zinc selenide with hydrocarbons. The surface tensions of the unentangled polymers, measured by pendant drop tensiometry, and the contact angles of these polymers on the zinc selenide surface are shown in Table 2. The surface attractions of the ordinary and deuterated polymers for zinc selenide are indistinguishable by these measurements. Surface segregation of isotopically labeled miscible polymers has been reported (Jones et al., 1990; Norton et al., 1995), but all our polymers are well below the molecular

Table 2. Surface-Tension Measurements

Liquid	Surface Tension [mN/m]	Contact Angle on ZnSe		
Hexadecane	26.9±0.2 (27.37)*	< 5°		
		1 min	5 min	10 min
h-PB1	27.2±0.2	20°	17°	17°
d-PB1	27.1±0.2	20°	17°	18°

*Interpolated to 22°C from literature data (Jasper, 1972).

weight necessary for preferential segregation of the deuterated polymer.

We cannot compute the polymer adsorption energy per segment because the surface energy of zinc selenide under our experimental conditions is not available. To obtain a relative value, we measured the surface tension and contact angle for hexadecane. Though hexadecane had a small contact angle, it did not completely wet the surface. (Hexane did wet.) Using the Young–Laplace equation, we can compute the difference ($\Delta\gamma$) between PB–ZnSe and hexadecane–ZnSe interfacial energies as

$$\Delta\gamma = \gamma_H \cos\Theta_H - \gamma_{PB}\cos\Theta_{PB} = 0.9 \text{ mN/m}, \quad (1)$$

where the H subscripts refer to hexadecane. If a polymer segment is about 7 Å long (Bates et al., 1986) and 3 Å wide, this surface-energy difference corresponds to about 0.05 kT/segment; that is, polybutadiene is slightly less attracted to the surface than is hexadecane.

We expect the difference in surface attraction to be the net result of competing entropic and enthalpic differences. Hexadecane is relatively short, so it suffers a smaller entropic penalty by being close to a surface. For a polymer, this entropic penalty has been estimated by lattice theory (Cohen Stuart et al., 1984) and by simulation (Matsuda et al., 1995) to be about 0.29 kT per segment. This difference in entropic repulsive forces is balanced by a difference in enthalpic attraction; the double bonds in polybutadiene should enhance its surface affinity. Based on a reported 25% increase in adsorption energy for butene relative to butane on silver (Pawela-Crew and Madix, 1995) and on activated carbon (Olivier et al., 1994), we estimate that the enthalpy of adsorption of polybutadiene on the zinc selenide surface is about 25% higher per segment than that of an alkane. Even if we assume that hexadecane suffers no entropic penalty at the surface, the total enthalpic attraction of polybutadiene to the surface is only $(0.29-0.05)\text{kT}\times 1.25/0.25 = 1.2$ kT/segment. For comparison, molecular dynamics simulations (Bitsanis and Pan, 1993) suggest that, in the melt, the near-surface dynamics do not become noticeably slowed by surface attraction until the segment-surface interaction energy is at least 2 kT/segment.

As a further test of the interaction of polybutadiene with the surface, we conducted a desorption experiment as follows. First, we deposited a 5% by weight solution of h-PB2 in hexane onto the zinc selenide surface, which was held at 25°C. After 15 min of equilibration, we flowed pure hexane, also at 25°C, at a rate of 0.82 mL/min through the flow cell and we monitored the desorption of the polybutadiene through the decay of the ATR/FTIR absorbance of the trans peak at 965 cm^{-1}, as shown in Figure 1. Though much of the signal comes

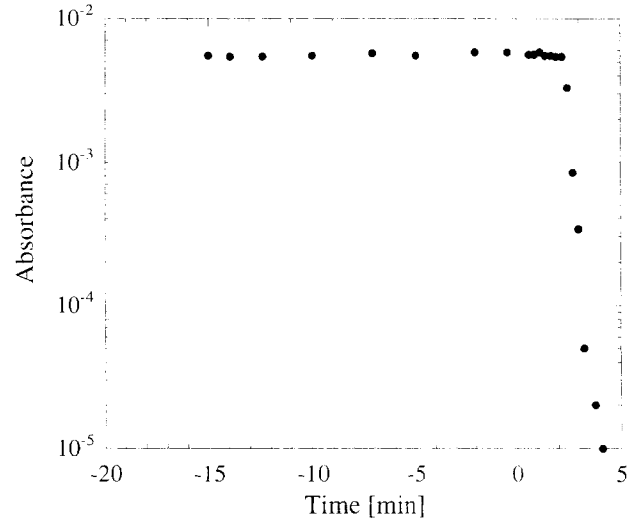

Figure 1. Desorption of polybutadiene into hexane.

from the bulk solution, whose signal decays quickly, the absorbance is still decreasing rapidly well below 3% of the initial absorbance. From literature data (Fetters et al., 1994; Brandrup and Immergut, 1987), we estimate that for this experiment, the ratio $d_p/(R_{EE}) = 600$ nm/18 nm, where d_p is the depth of penetration of the evanescent wave (Mirabella, 1993), and R_{EE} is the mean-square end-to-end distance of the polybutadiene chain in a good solvent. Therefore, an absorbance of 3% of the initial value would be equivalent to the absorbance of a 5% polymer solution of thickness equal to the polymer end-to-end distance. Because the signal is still decaying well below this threshold, we can conclude that the near-surface chains can be desorbed easily, and thus the interaction with the surface is not strong. In contrast, polymers adsorbed from solution onto strongly attractive surfaces have very long time scales of desorption, and in some cases adsorb irreversibly (Pefferkorn et al., 1985; Dijt et al., 1992; Douglas et al., 1994).

Rheology

The dynamical rheological properties of h-PB2 were measured with a Rheometrics RMS 800 dynamic mechanical spectrometer using a 0.04-radian truncated cone-and-plate geometry. The storage (G') and loss (G'') moduli vs. oscillation frequency (ω) at a strain amplitude of 200% are shown in Figure 2, together with the magnitude of the complex viscosity, η^*, defined as

$$|\eta^*| = \left[\left(\frac{G'}{\omega}\right)^2 + \left(\frac{G''}{\omega}\right)^2\right]^{1/2}, \quad (2)$$

where $|\eta^*|$ should equal the steady shear viscosity at a shear rate $\dot{\gamma} = \omega$ for simple polymers (Cox and Merz, 1958). The measured zero-shear viscosity at 25°C was 52 Pa·s, in good agreement with literature data (Colby et al., 1987) for 1,4-polybutadiene of this molecular weight. Although the polymer is considered entangled above $M_e = 2-3\ M_e$, or about 4,000 g/mol (Colby et al., 1987), the relaxation time (~ 0.04

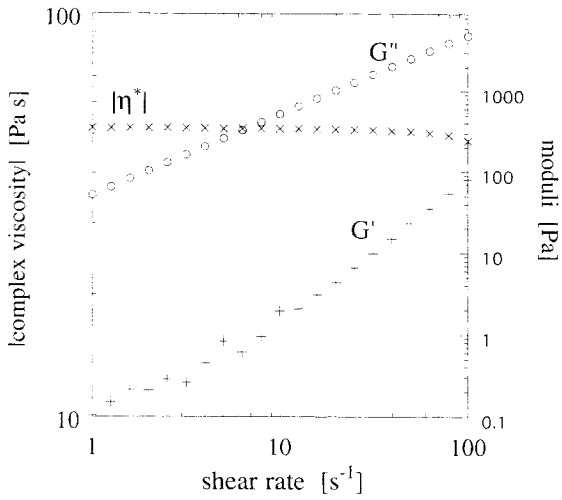

Figure 2. Dynamical rheological properties of h-PB2.

ms) was too short to observe in the rheometer. Figure 2 also shows that the viscosity was only a weak function of shear rate, allowing us to approximate the velocity profile as Newtonian for our analysis and simulations without appreciable error.

Experimental Studies

The experimental setup has been described in detail by Dietsche (1993) and David (1994). A brief description, including some minor modifications, is given below.

Optics

Our Mattson Polaris spectrometer was modified for ATR use by the addition of a special mirror assembly purchased from Harrick Scientific. The mirrors direct the light from a polychromatic, water-cooled Glowbar source to a zinc selenide ATR crystal (Spectra-Tech). The angle of the flat surface of the crystal relative to the incident light could be set by means of a caliper. Using atomic force microscopy, we found that the flat surface was surprisingly smooth; the root-mean-square roughness of the surface was 4.3 Å. Since half of the curved surface of the ATR crystal was coated with aluminum, the light internally reflects twice from the flat surface before reflecting from the remaining mirrors and reaching the mercury–cadmium–telluride detector. Because sampling near the side walls (where the velocity is much less than the center-line velocity) would create the illusion of slow near-surface dynamics, a mask was inserted in the light path near the crystal, as shown in Figure 3.

Flow apparatus

The flow system is depicted in Figure 4. A 0.79-cm-long, 0.62-cm-wide and 0.066-cm-deep groove was machined into a stainless-steel block to create a rectangular flow channel when the zinc selenide ATR crystal is clamped to the block with a Viton O-ring seal. The rectangular flow channel is connected to the external piping [1/4-in. (6.35-mm) stainless-steel Swagelok] through slanting entrance and exit regions. The d-PB was introduced into the flow channel via a syringe at-

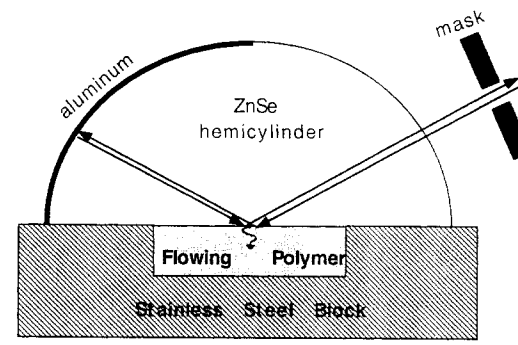

Figure 3. Attenuated total reflection optics.

tached to a four-way valve. For pressure drops less than 10 psi, an infusion pump was used to deliver h-PB at a constant rate. For higher pressure drops, the flow of h-PB was driven from a reservoir by regulated nitrogen pressure (not shown). When the flow was driven by nitrogen pressure, the flow rate was determined by collecting the effluent from the spectrometer for 2 or 3 min in a tared scintillation vial, then weighing the contents. Four temperature control loops were used to maintain the temperature at 30 ± 0.2°C in the h-PB reservoir, the four-way valve, the inlet pipe, and the stainless-steel block. Temperatures were measured with OMEGA type-J thermocouples placed throughout the flow system. The controller outputs were sent to Thermolyne heating tapes wrapped around the piping system as well as through a cartridge heater inserted into a drilled hole in the stainless-steel block.

Experimental protocol

Before each experiment, the ATR crystal was cleaned with hot distilled hexane for several hours, then dried with flowing nitrogen. All experiments were run with the flat surface of the ATR crystal at a constant angle of about 54° relative to the incident light beam. At this angle, the evanescent wave intensity decays to $1/e$ of its surface value at a penetration

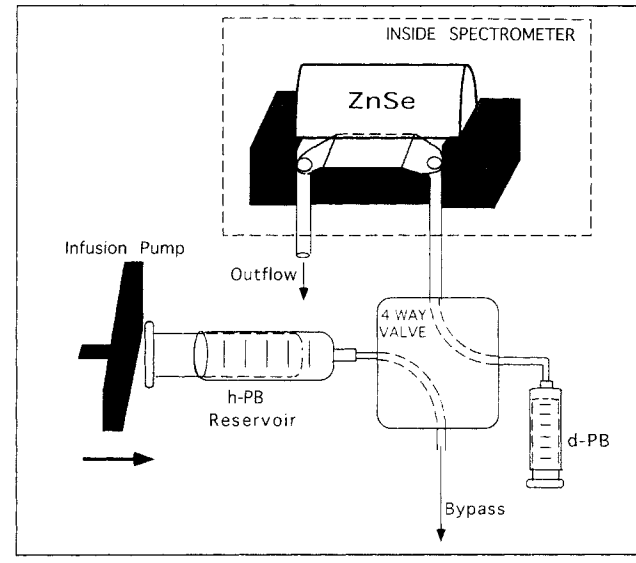

Figure 4. Flow system.

depth of about 290 nm for a wavenumber of 2,210 cm^{-1} (Mirabella, 1993; Driscoll, 1978). Before each experiment, a background of the empty flow channel was taken, then the d-PB was injected into the flow channel and its spectrum was taken. Next, we started the flow of h-PB through the four-way valve, bypassing the flow system. At time $t = 0$, the four-way valve was switched to allow flow of h-PB to replace the d-PB in the flow channel. Toward the end of some experiments, a portion of the polymer exiting the flow system was collected for SEC analysis. In all cases, the SEC elution curves were identical before and after flow through the apparatus, indicating that the polymers did not suffer cross-linking or chain scission during the experiments.

We report our results in terms of the normalized absorbance of d-PB, which is defined as the ratio of the net height of the C-D stretch at 2,210 cm^{-1} at any time to that of the pure d-PB. The net peak height at 2,210 cm^{-1} was calculated using the absorbances in stable, nonabsorbing regions of the IR spectrum (2,300 cm^{-1} and 1,940 cm^{-1}) to form a base line. Since the refractive indices of deutero- and protio-compounds are very close, we did not attempt to correct for the change in refractive-index matching with concentration. The signal-to-noise ratio is about 1,000 for the pure deuterated polybutadiene melt.

Results

The experiments with $M \sim 1{,}500$ g/mol polymers are shown in Figure 5. The experiments differ in the syringe-driven flow rate of h-PB as indicated in the figure. In all four experiments, the absorbance of d-PB approximates a delay plus a first-order decay, as expected for uniform Fickian diffusion.

Three different pressure-driven flow rates were used for the entangled polymers (Figure 6). The experiment at 6.1 mL/min was halted prematurely when nitrogen was sucked into the flow system. Since the highest wall stress encountered (at a flow rate of 6.1 mL/min, corresponding to a wall shear rate of 240 s^{-1}) was only about 0.01 MPa, or less than 1% of the plateau modulus (Fetters et al., 1994), slip was not expected to occur in these experiments (Denn, 1990, 1994; Hatzikiriakos and Dealy, 1991).

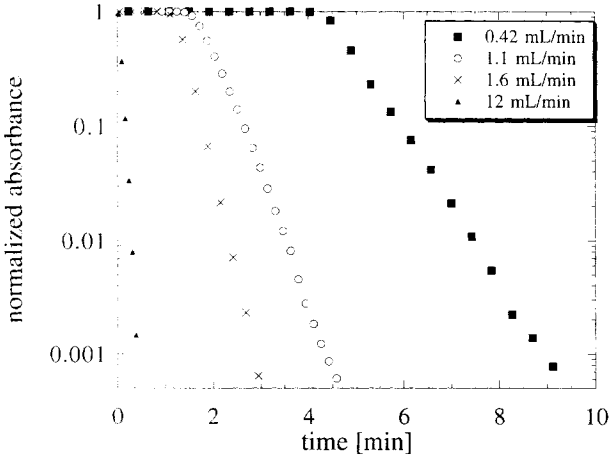

Figure 5. Decay profiles of unentangled polymers.

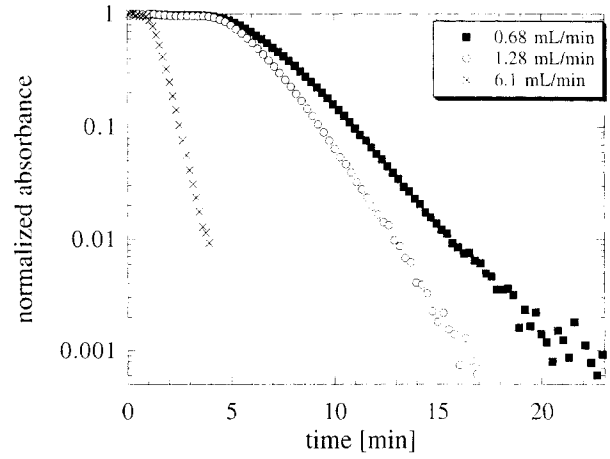

Figure 6. Decay profiles of entangled polymers.

Simulations

The experiments just described were simulated as a transient, three-dimensional convection-diffusion problem using FIDAP 7.0, a finite-element package (Fluid Dynamics, Inc.). The simulation geometry used to approximate the experimental geometry is shown in Figure 7. The equations of momentum and mass transfer were decoupled; FIDAP first calculated the steady-state velocity profile for a Newtonian fluid, which was then fed into the transient convection–diffusion simulation. The evolution of the concentration profile with time for typical experimental conditions is shown in Figure 8 for a line of nodes along the center line, 4 mm downstream of the beginning of the rectangular flow channel. Note that the concentration profile is flat within a micrometer of the surface at all times. For all experimental conditions, the near-surface concentration profile was sufficiently flat to equate the normalized ATR absorbance to the normalized concentration at $y = 0$. We also found that near the center line, the time-scale of the decay depended only weakly on the position in both the flow and vorticity directions. Therefore, the experimental results should not be distorted by the finite IR beam area.

Because of the high Peclet numbers involved, convergent solutions with FIDAP were difficult to obtain for diffusivities below 5×10^{-10} m^2/s at flow rates near 1 mL/min. This

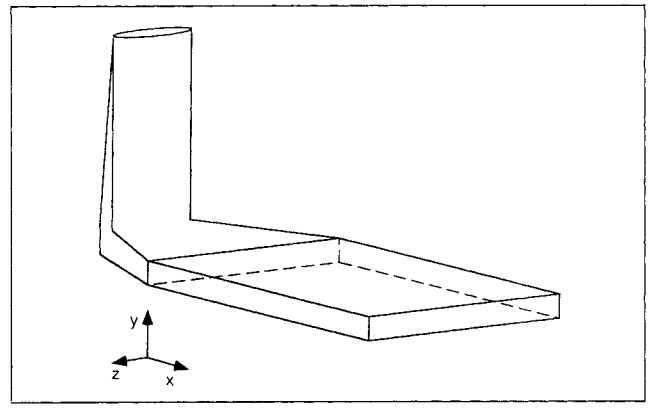

Figure 7. Geometry for finite-element simulation.

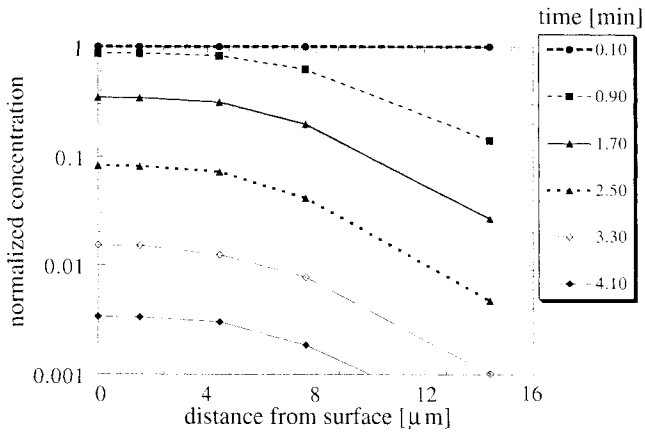

Figure 8. Concentration profiles from finite-element simulation.

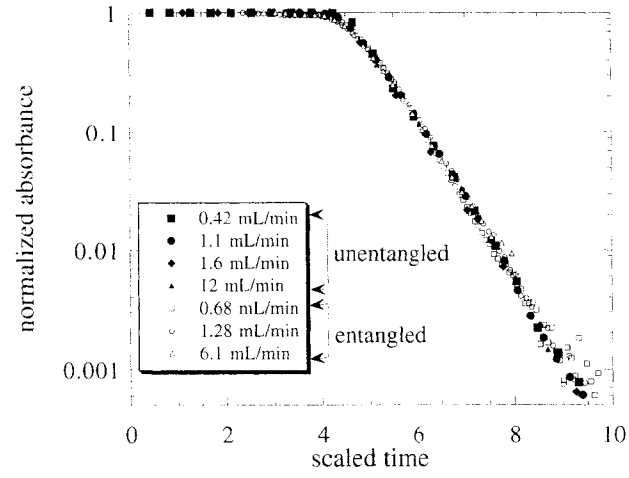

Figure 10. Time-scaled experimental results.

problem was somewhat alleviated by using an artificially high diffusivity (3×10^{-6} m^2/s in the direction of flow, 3×10^{-8} m^2/s perpendicular to this direction) for nodes more than 50 μm from the ATR surface. However, even after this modification, for diffusivities less than 10^{-10} m^2/s, some regions of the mesh reached concentrations greater than 1.1 or less than -0.1 before attaining zero concentration. We therefore used a scaling analysis to compare to experiments at higher Peclet numbers. If the mass-transfer boundary layer is much smaller than the half-thickness of the flow channel, then the characteristic time for a one-dimensional flow should scale as (Lok et al., 1983; Shibata and Lenhoff, 1992)

$$t^* \sim D^{-1/3}\dot{\gamma}_w^{-2/3}, \tag{3}$$

where $\dot{\gamma}_w$ is the shear rate at the wall and D is the diffusivity of the melt. For Newtonian flow, the wall shear rate can be replaced by the flow rate in the preceding scaling relation. The details of the scaling argument are contained in the Appendix.

Since FIDAP could not be used for the high Peclet numbers associated with our flow rates and diffusivities, we developed a three-dimensional finite difference scheme incorporating the lubrication approximation for the velocity in nonplanar sections to test the accuracy of Eq. 3 for our range of experimental conditions. Several runs of the code at the same flow rate (0.63 mL/min) with different diffusivities are shown in Figure 9; these demonstrate that the scaling analysis is reasonably accurate throughout the range of experimental conditions, enabling us to extrapolate the FIDAP results to our experimental conditions using Eq. 3.

Analysis

In the absence of slow surface dynamics, the shapes of the decay curves from different experiments should be identical. We were able to collapse all experiments onto a single curve by scaling the time axis of each run by appropriate multiplicative factors, as shown in Figure 10. The dependence of these factors on flow rate and molecular weight is shown in Figure 11; the lines of slope $-2/3$ denote the expected scaling with flow rate from Eq. 3. The agreement with the $Q^{-2/3}$

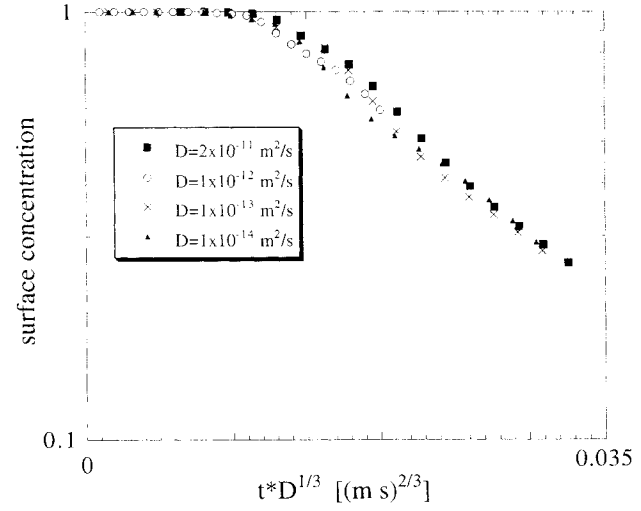

Figure 9. Scaling of simulations with diffusivity.

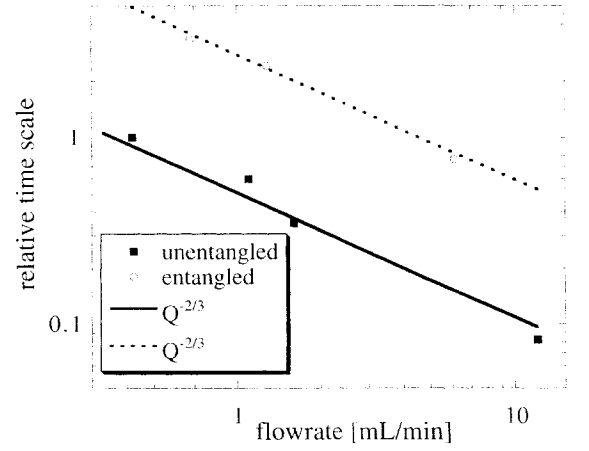

Figure 11. Scaling of characteristic time with flow rate.

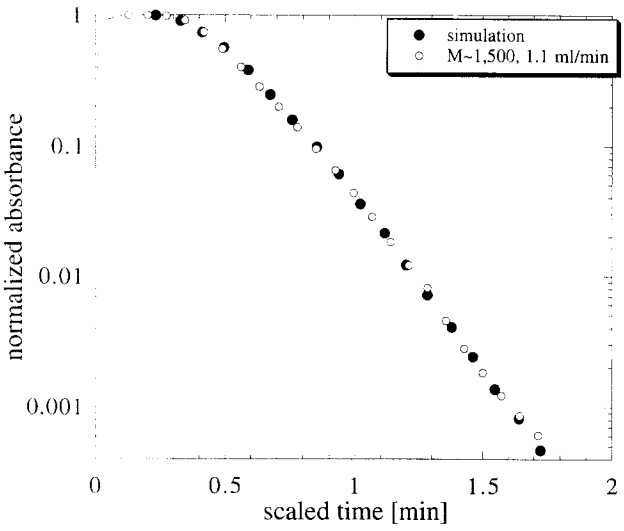

Figure 12. Comparison to finite-element simulation.

scaling is very good, with somewhat more scatter for the unentangled polymers.

The decay curves also match well to a time-scaled FIDAP simulation, as shown in Figure 12 for one of the unentangled runs. We extracted diffusivities from the experimental data using Eq. 3 and the scaling factors necessary to match the experimental decay curves to the simulation. These extracted diffusivities are shown in Figure 13, as well as diffusivities calculated with the empirical equation of Pearson et al. (1994)

$$D = \frac{\rho RT\langle R_{EE}^2\rangle}{36\eta M}\left[1+\left(\frac{M}{9.5M_e}\right)^{1.5}\right] \tag{4}$$

using reported viscosities, densities, and chain dimensions (Colby et al., 1987; Fetters et al., 1994). Equation 4 is valid in the crossover region and reduces to the Rouse model for unentangled polymers. For the unentangled polymer, we obtain a value of $D = 3.0\times10^{-12}$ m^2/s, while for $M = 15{,}000$ we obtain $D = 2.0\times10^{-14}$ m^2/s using a viscosity of 45 Pa·s at $T =$ 30°C. The value for the entangled polymer is in good agreement with the data of Fleischer and Appel (1995) adjusted to 30°C by assuming the product ηD is independent of temperature. Much of the error in the diffusivities estimated from experiments arises from uncertainty in the experimental geometry, which influences the characteristic time of the decay curve. The diffusivity calculations are quite sensitive to errors in time-scaling; a 15% error in time scaling yields a 52% error in the estimated diffusivity.

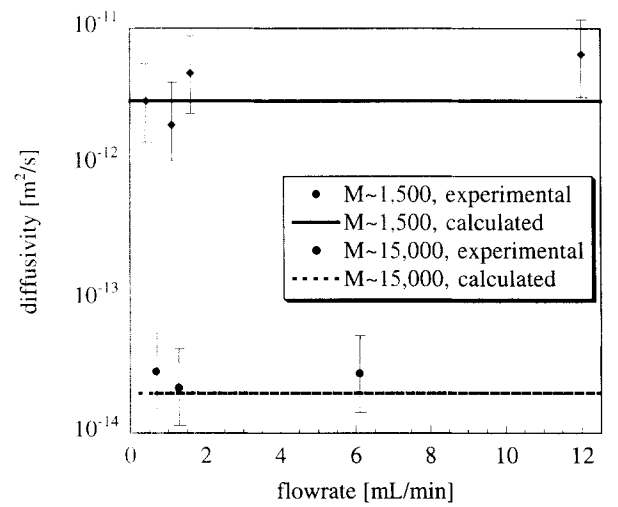

Figure 13. Estimated diffusivities.

Discussion

In all cases, the near-surface dynamics were consistent with flow-rate-independent, uninhibited near-surface diffusion in the direction normal to the surface. However, because the distance over which diffusion occurs (2–15 μm) is much greater than the polymer dimensions (R_{EE} = 2–10 nm) (Fetters et al., 1994), the experiments are unable to detect a near-surface retardation of dynamics unless the retardation is extremely pronounced or the near-surface region is much greater than the polymer dimensions. As a rough estimate, the near-surface dynamics will become apparent when the characteristic time for diffusion in the near-surface region becomes comparable to the characteristic time for diffusion in the mass-transfer boundary layer. Since the characteristic time for diffusion over a distance Δy scales as $(\Delta y)^2$, the effective diffusivity of a near-surface region of width R_{EE} would need to be a factor of at least $(1{,}000)^2 = 10^6$ less than the bulk diffusivity to create noticeably slow near-surface dynamics in our experiments. This is a much greater factor than predicted from simulations (Mansfield and Theodorou, 1989; Bitsanis and Pan, 1993; Shaffer, 1996) or reported in other experiments (Zheng et al., 1995; Van Alsten et al., 1992). Because smaller chains have smaller dimensions and higher diffusivities, the ratio of diffusion length to R_{EE} increases with decreasing chain length, requiring the ratio of bulk-to-surface-region diffusivities to be even greater than 10^6 to create an observable effect for a surface monolayer of smaller chains.

In light of the preceding, we must conclude that the previous results (Dietsche et al., 1995; David et al., 1995) with hexadecene/hexadecane were indicative of extremely slow near-surface dynamics, orders of magnitude slower than reported in simulations. To confirm those results, we repeated the experiments with C_{16}'s on the same surface as the PB experiments outlined earlier. As shown in Figure 14, the hexadecene decay curve is strikingly different from that of the unentangled d-PB for similar flow rates. The long-time sluggish decay of the hexadecene signal indicates that some of the molecules in the near-surface region have very slow dynamics, even though we expect that hexadecene's paucity of double bonds results in a weaker enthalpic interaction with the zinc selenide surface than for polybutadiene. We therefore conclude that the wall induces slower near-surface dynamics of C_{16}'s even in the absence of significant segment-surface attractions. Furthermore, the slowdown of the hexadecene decay rate occurs at an absorbance equivalent to a thickness much greater than a monolayer coverage on the surface. Though the mechanism underlying the extremely slow near-surface dynamics of C_{16}'s is still unknown, we believe it may indicate a tendency of short, crystallizable molecules near

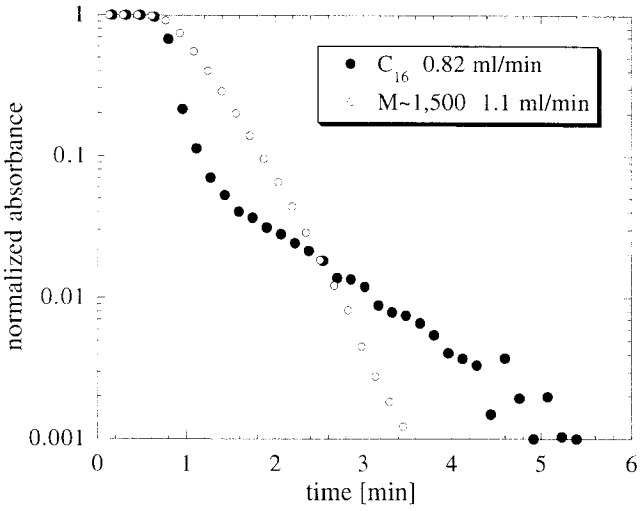

Figure 14. Comparison of decay profiles of $M \sim 1{,}500$ to C_{16}.

a surface to form a more ordered structure that is several monolayers thick. We believe that we do not observe this effect for the polybutadienes because they are longer, noncrystallizable chains; hence, they are unable to form a surface layer with detectably slower dynamics than in the bulk.

Conclusions

For both unentangled and entangled linear amorphous polybutadiene, the relaxation of a concentration gradient of isotopically labeled chains is consistent with uninhibited diffusion normal to the surface for near-surface chains under mild flow conditions. This is in direct contrast to previous studies of shorter, crystallizable molecules (C_{16}'s), which showed surprisingly long-time scales in similar experiments.

Acknowledgment

This work was supported by the Director, Office of Energy Research, Office of Basic Energy Sciences, Materials Science Division of the U.S. Department of Energy under Contract No. DE-/AC03-76SF00098. Geoffrey Wise received fellowship support from the National Science Foundation.

Literature Cited

Atkin, E. L., L. A. Kleintjens, and R. Koningsveld, "Liquid-Liquid Phase Separation in Multicomponent Polymer Systems; Deuterium Isotope Effect in Polymer Compatibility," *Makromol. Chem.*, **185**, 377 (1984).

Bates, F. S., H. Bair, and M. A. Hartney, "Block Copolymers near the Microphase Separation Transition. 1. Preparation and Physical Characterization of a Model System," *Macromol.*, **17**, 1987 (1984).

Bates, F. S., S. B. Dierker, and G. D. Wignall, "Phase Behavior of Amorphous Binary Mixtures of Perdeuterated and Normal 1,4-Polybutadienes," *Macromol.*, **19**, 1938 (1986).

Bates, F. S., and P. Wiltzius, "Spinodal Decomposition of a Symmetric Critical Mixture of Deuterated and Protonated Polymer," *J. Phys. Chem.*, **91**, 3258 (1989).

Bitsanis, I., and C. Pan, "The Origin of 'Glassy' Dynamics at Solid-Oligomer Interfaces," *J. Chem. Phys.*, **7**, 5520 (1993).

Bitsanis, I., and G. ten Brinke, "A Lattice Monte Carlo Study of Long Chain Conformations at Solid-Polymer Melt Interfaces," *J. Chem. Phys.*, **99**, 3100 (1993).

Brandrup, J., and E. Immergut, *Polymer Handbook*, 3rd ed., Wiley, New York (1987).

Brochard, F., and P. G. de Gennes, "Shear Dependent Slippage at a Polymer-Solid Interface," *Langmuir*, **8**, 3033 (1992).

Carella, J. M., W. W. Graessley, and L. J. Fetters, "Effects of Chain Microstructure on the Viscoelastic Properties of Linear Polymer Melts: Polybutadienes and Hydrogenated Polybutadienes," *Macromol.*, **17**, 2775 (1984).

Cohen Stuart, M. A., G. J. Fleer, and J. M. H. M. Scheutjens, "Displacement of Polymers I. Theory," *J. Coll. Interf. Sci.*, **97**, 526 (1984).

Colby, R. H., L. J. Fetters, and W. W. Graessley, "Melt-Viscosity-Molecular Weight Relationships for Linear Polymers," *Macromol.*, **20**, 2226 (1987).

Cox, W. P., and E. H. Merz, "Correlation of Dynamic and Steady Flow Viscosities," *J. Poly. Sci.*, **28**, 118 (1958).

David, C., "Flow-Induced Surface Exchange Kinetics," MS Thesis, Univ. of California at Berkeley (1994).

David, C., M. M. Denn, and A. T. Bell, "Dynamics of Flow-Induced Surface Exchange," *Ind. & Eng. Chem. Res.*, **34**, 3336 (1995).

Denn, M. M., "Issues in Viscoelastic Fluid Mechanics," *Annu. Rev. Fluid Mech.*, **22**, 13 (1990).

Denn, M. M., "Polymer Flow Instabilities: A Picaresque Tale," *Chem. Eng. Educ.*, **28**, 162 (1994).

Dietsche, L. J., "Surface Interactions in a Shear Field," PhD Diss., Univ. of California at Berkeley (1993).

Dietsche, L. J., M. M. Denn, and A. T. Bell, "Surface Interactions in a Shear Field," *AIChE J.*, **41**, 1266 (1995).

Dijt, J. C., M. A. Cohen Stuart, and G. J. Fleer, "Kinetics of Polymer Adsorption and Desorption in Capillary Flow," *Macromol.*, **25**, 5416 (1992).

Douglas, J. F., P. Frantz, H. E. Johnson, H. M. Schneider, and S. Granick, "Regimes of Polymer Adsorption-Desorption Kinetics," *Coll. and Surf. A*, **86**, 251 (1994).

Driscoll, W., *Handbook of Optics*, McGraw-Hill, New York (1978).

Fetters, L., D. J. Lohse, D. Richter, T. A. Witten, and A. Zirkel, "Review: Connection between Polymer Molecular Weight, Density, Chain Dimensions and Melt Viscoelastic Properties," *Macromol.*, **27**, 4639 (1994).

Fleischer, G., and M. Appel, "Chain Length and Temperature Dependence of the Self-Diffusion of Polyisoprene and Polybutandiene in the Melt," *Macromol.*, **28**, 7281 (1995).

Hatzikiriakos, S. J., and J. M. Dealy, "Wall Slip of Molten High Density Polyethylene I. Sliding Plate Rheometer Studies," *J. Rheol.*, **35**, 497 (1991).

Jasper, J. J., "The Surface Tension of Pure Liquid Compounds," *J. Phys. Chem. Ref. Data*, **1**, 841 (1972).

Jinnai, H., H. Hasegawa, T. Hashimoto, and C. Han, "Time-Resolved Small-Angle Neutron Scattering Study of Spinodal Decomposition in Deuterated and Protonated Polybutadiene Blends," *J. Chem. Phys.*, **99**, 4845 (1993).

Jones, R. A., L. J. Norton, E. J. Kramer, R. J. Composto, R. S. Stein, T. P. Russell, A. Mansour, A. Karim, G. P. Felcher, M. H. Rafailovich, J. Sokolov, Z. Zhao, and S. A. Schwarz, "The Form of the Enriched Surface Layer in Polymer Blends," *Europhys. Lett.*, **12**, 41 (1990).

Kumar, S., and T. P. Russell, "Behavior of Isotopic, Binary Polymer Blends in the Vicinity of Neutral Surfaces: The Effects of Chain-Length Disparity," *Macromol.*, **24**, 2816 (1991).

Larson, R. G., "Instabilities in Viscoelastic Flows," *Rheol. Acta*, **31**, 213 (1992).

Lok, B. K., Y.-L. Cheng, and C. R. Robertson, "Total Internal Reflection Fluorescence: A Technique for Examining Interactions of Macromolecules with Solid Surfaces," *J. Coll. Interf. Sci.*, **91**, 87 (1983).

Mansfield, K., and D. N. Theodorou, "Interfacial Structure and Dynamics of Macromolecular Liquids: A Monte Carlo Simulation Approach," *Macromol.*, **22**, 3143 (1989).

Matsuda, T., G. Smith, R. Winkler, and D. Yoon, "Stochastic Dynamics Simulations of n-Alkane Melts Confined between Solid Surfaces: Influence of Surface Properties and Comparison with Scheutjens-Fleer Theory," *Macromol.*, **28**, 165 (1995).

Mirabella, F., *Internal Reflection Spectroscopy*, Dekker, New York, (1993).

Ndoni, S., C. M. Papadakis, F. S. Bates, and K. Almdal, "Labora-

tory-Scale Setup for Anionic Polymerization under Inert Atmosphere," *Rev. Sci. Instrum.*, **66**, 1090 (1995).
Norton, L. J., E. J. Kramer, F. S. Bates, M. D. Gehlsen, R. A. Jones, A. Karim, G. P. Felcher, and R. Kleb, "Neutron Reflectometry Study of Surface Segregation in an Isotopic Poly(ethylenepropylene) Blend: Deviation from Mean Field Theory," *Macromol.*, **28**, 8621 (1995).
Olivier, M.-G., K. Berlier, and R. Jadot, "Adsorption of Butane, 2-Methylpropane, and 1-Butene on Activated Carbon," *J. Chem. Eng. Data*, **39**, 770 (1994).
Pan, C., and I. Bitsanis, "Structure, Conformation, and Dynamics of Polymer Chains at Solid Melt Interfaces," *Makromol. Chem.* **65**, 211 (1993).
Pawela-Crew, J., and R. J. Madix, "Lateral Interactions in the Desorption Kinetics of Weakly Adsorbed Species: Unexpected Differences in the Desorption of C4 Alkenes and Alkanes from Ag(110) Due to Oriented Pi-Bonding of the Alkenes," *Surf. Sci.*, **339**, 8 (1995).
Pearson, D. S., L. J. Fetters, W. W. Graessley, G. Ver Strate, and E. von Meerwall, "Viscosity and Self-Diffusion Coefficient of Hydrogenated Polybutadiene," *Macromol.*, **27**, 711 (1994).
Pefferkorn, E., A. Carroy, and R. Varoqui, "Dynamic Behavior of Flexible Polymers at a Solid/Liquid Interface," *J. Polym. Sci.: Polym. Phys.*, **23**, 1997 (1985).
Shaffer, J. S. "Dynamics of Confined Polymer Melts: Topology and Entanglement," *Macromol.*, **29**, 1010 (1996).
Shibata, C. T., and A. M. Lenhoff, "TIRF of Salt and Surface Effects on Protein Adsorption II. Kinetics," *J. Coll. Interf. Sci.*, **148**, 485 (1992).
Van Alsten, J. G., B. B. Sauer, and D. Walsh, "Polymer Dynamics at the Melt/Solid Interface: Experimental Evidence of Reduced Center of Mass Mobility," *Macromol.*, **25**, 4046 (1992).
Van der Velden, G. P. M., and L. J. Fetters, "Microstructure Determination of Nondeuterated, Partially Deuterated, and Perdeuterated PBs with Cis-1,4 Trans-1,4, and Vinyl-1,2 Units by 13C NMR," *Macromol.*, **23**, 2470 (1990).
Wang, S.-Q., P. A. Drda, and Y.-W. Inn, "Exploring Molecular Origins of Sharkskin, Partial Slip, and Slope Change in Flow Curves of Linear Low Density Polyethylene," *J. Rheol.*, **40**, 875 (1996).
Zheng, X., B. B. Sauer, J. G. Van Alsten, S. A. Schwartz, M. H. Rafailovich, J. Sokolov, and M. Rubinstein, "Reptation Dynamics of a Polymer Melt Near an Attractive Solid Interface," *Phys. Rev. Lett.*, **74**, 407 (1995).

Appendix: Approximate Scaling Analysis

Problem statement

To predict the effect of flow rate and diffusivity on the decay curves seen in the experiments, a simple scaling analysis can be developed for the case of a uniform diffusivity D and a simplified flow geometry. As shown in Figure A1, the flow system is simplified by approximating the velocity profile as uniform in the flow direction, and ignoring any dependence on the vorticity (z) direction. The general transport equation for this system is

$$\frac{\partial c}{\partial t} = -v_x(y)\frac{\partial c}{\partial x} + D\frac{\partial^2 c}{\partial y^2}, \tag{A1}$$

where the diffusional term in the flow direction has been neglected for large Peclet numbers. The half-height of the flow slit was 330 μm, while the region of interest was $y < 30$ μm; in this near-wall region the velocity can be approximated as linear, and the transport equation becomes

$$\frac{\partial c}{\partial t} = -\dot{\gamma}_w y\frac{\partial c}{\partial x} + D\frac{\partial^2 c}{\partial y^2}, \tag{A2}$$

where $\dot{\gamma}_w$ is the shear rate at the wall.

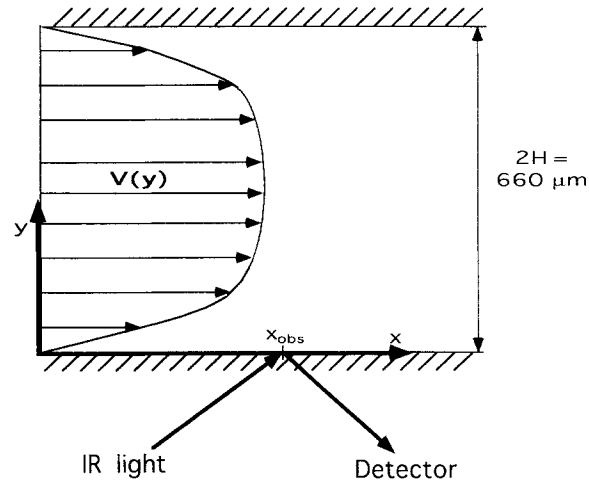

Figure A1. Geometry for scaling analysis.

The experimental boundary conditions are inflow of pure h-PB:

$$c = 0 \quad \text{at} \quad x = 0, \qquad t > 0 \tag{A3}$$

and no flux of d-PB through the ATR crystal:

$$\frac{\partial c}{\partial y} = 0 \quad \text{at} \quad y = 0. \tag{A4}$$

Because of the boundary-layer assumption, the second boundary condition in the shear direction should be written as

$$c = 0 \quad \text{at} \quad y = \infty. \tag{A5}$$

The initial condition is pure d-PB in the flow cell at $t = 0$, or

$$c = 1 \quad \text{at} \quad t = 0, \qquad x > 0. \tag{A6}$$

Scaling

We are interested in the solution of the differential equation near the surface at a fixed observation location $x = x_{obs}$, corresponding to the position in the flow direction where the infrared beam reflects at the crystal–polymer interface. The following choices of dimensionless variables (Lok et al., 1983) remove all parameters from the problem:

$$X = x/x_{obs} \tag{A7}$$

$$Y = y\Big/\left(\frac{Dx_{obs}}{\dot{\gamma}_w}\right)^{1/3} \tag{A8}$$

and

$$T = t \Big/ \left(\frac{x_{\text{obs}}^2}{D\dot{\gamma}_w^2} \right)^{1/3}. \tag{A9}$$

Therefore, in nondimensional form, the transport equation is

$$\frac{\partial c}{\partial T} = -Y\frac{\partial c}{\partial X} + \frac{\partial^2 c}{\partial Y^2}. \tag{A10}$$

The near-surface concentration profiles will be identical from experiment to experiment if distance from the surface and time are scaled as in Eqs. A8 and A9.

The initial boundary-layer thickness for all experiments was at least 6 d_p; we can equate normalized absorbance with normalized concentration at the surface because the concentration profile is close to the wall value over a substantial fraction of the boundary layer. As convection brings the concentration step toward the surface, however, the mass-transfer boundary layer decreases from its initial value, steepening the concentration gradient. For most runs, the boundary layer was larger than the penetration depth for all experimental times; only in the entangled run at 6.1 mL/min did the boundary layer approach d_p toward the end of the experiment.

Manuscript received July 7, 1997, and revision received Dec. 10, 1997.